CHEMICAL ENGINEERING TRANSACTIONS
VOL. 74, 2019
A publication of AIDIC
The Italian Association of Chemical Engineering
Online at www.cetjournal.it
Guest Editors: Sauro Pierucci, Jiří Jaromír Klemeš, Laura Piazza

ISBN 978-88-95608-71-6; **ISSN** 2283-9216
DOI: 10.3303/CET1974073

Novel Synthesis of Mixed Oxide Nanoparticles for Photocatalysis

Miguel Sanchez Mendez, Khley Cheng, Khay Chhor, Mamadou Traore, Mounir Ben Amar, Andrei Kanaev*

Laboratoire des Sciences des Procédés et des Matériaux, CNRS, Université Paris 13, Sorbonne Paris Cité, 93430 Villetaneuse, France
andrei.kanaev@lspm.cnrs.fr

Vanadium oxo-alkoxy nanoparticles were prepared via sol-gel method, manually and in a chemical reactor with ultra-rapid micromixing. The materials were characterized by DLS, ATG-ATD, XRD and SEM methods. The influence of micromixing conditions on the particle size and growth kinetics was evaluated. Complementary, the preparation of mixed-oxide nanoparticles in presence of vanadium and titanium precursors was performed, showing a strong interaction between the two systems, promising for the fabrication of size- and compositional selective Ti-V oxide nanoparticles for photocatalysis.

1. Introduction

Natural resources have reached nowadays a high level of pollution, between which air and water pollution contribute most important in the balance of the ecosystem. The pollutants are usually toxic organic compounds like dyes, detergents and surfactants, agro wastes like insecticides and herbicides, etc. In order to solve this problem, the development of clean and green processes is under way, among which photocatalysis takes a special place (Fox and Dualy, 1993; Ohtani, 2010).
One of most effective photocatalysts, TiO_2, has been a subject of numerous studies since many decades (Hashimoto et al., 2005; Schneider et al., 2014; Fagan et al., 2016; Chianese et al., 2017; Lovino et al., 2019). Because of rather high band gap energy, i.e. E_g=3.0-3.2 eV, this material cannot be activated with visible light. Consequently, many studies have been performed to decrease its absorption onset by the compositional modification. Another issue in preparation of an effective photocatalyst concerns the decrease of the photoinduced charges recombination, whose solution can be found in preparing composites of TiO_2 with other metal oxides, as e.g. TiO_2-ZrO_2 (Reddy and Khan, 2007). One of important problems in this respect is the control of its compositional homogeneity at nanoscale, since inhomogeneous domains and elements clustering can affect material properties and effectiveness in the photocatalytic process (Tieng at al., 2011).
Vanadium pentoxide (V_2O_5) is one relevant material with semiconducting properties and relatively narrow bang-gap E_g=2.2 eV, which could be potentially used in photocatalysis with the visible light activation (Kruef et al., 2017; Li et al., 2006). However, a high probability of the photogenerated electron-hole pair recombination was a serious drawback limiting its effectiveness. A possible solution to overcome this problem is to prepare mixed-oxide materials. Several compositions of V_2O_5 with other semiconductors have been realized so far: V_2O_5/SiO_2 (Amano et al., 2004), V_2O_5/$BiVO_4$ (Su et al., 2011), V_2O_5/Al_2O_3 (Teramura et al., 2009) and TiO_2/V_2O_5 (Jianhua et al., 2006), which have not been effective in the photocatalytic process. However, as it has been recently shown (Cheng et al., 2018), an effective mixed-oxide photocatalysts can be prepared following a bottom-up approach from size- and composition- selected nanoparticles by controlling their nucleation-growth process in chemical reactors with ultra-rapid micromixing (Azouani et al., 2009; Azouani et al., 2010). In particular, mixing of most effective titanium oxide with vanadium oxide at the molecular level may lead to the nucleation of the mixed-oxide nanoparticles that permits preparation of novel effective photocatalysts with the visible light activation. An evaluation of the ternary Ti-V-O system via thermodynamic CALPHAD modeling (Yang et al., 2017) has predicted several stable compositions, which needs further experimental verification. In

Paper Received: 23 June 2018; Revised: 4 December 2018; Accepted: 17 February 2019

Please cite this article as: Sanchez Mendez M., Cheng K., Chhor K., Traore M., Ben Amar M., Kanaev A., 2019, Novel Synthesis of Mixed Oxide Nanoparticles for Photocatalysis , Chemical Engineering Transactions, 74, 433-438 DOI:10.3303/CET1974073

present communication, we report on the influence of micromixing conditions on nucleation-growth of vanadium oxide and mixed oxide Ti-V nanoparticles. The synthesis was achieved using sol-gel method either manually or in a chemical reactor with ultra-rapid micromixing. Improved particle size homogeneity and interaction between titanium and vanadium oxide species were shown in the micromixing conditions at the nucleation stage.

2. Experimental

2.1 Material preparation

The metal oxide nanoparticles, either single oxide vanadium oxo-alkoxy (VOA) and titanium oxo-alkoxy (TOA) or mixed-oxide vanadium-titanium-oxo-alkoxy (VTOA), were prepared in this study via sol-gel method either manually with a magnetic stirring or in a chemical reactor with ultra-rapid micromixing. The reactor used for the synthesis of the metal oxide nanoparticles has been described in our previous studies (Rivalin et al., 2005, Azouani et al., 2010). In brief, two solutions of 50 mL each containing A) precursors of vanadium(V) oxytripropoxide (98%, Sigma Aldrich) in n-propanol (99.5%, Sigma Aldrich) and B) distilled water filtered twice (syringe filter 0.1 µm porosity PALLs Acrodisc) in n-propanol were prepared in a LABstar glove box workstation MBraun (O_2≤80 ppm, H_2O≤0.5 ppm), in order to avoid any contamination by air humidity and dust particles promoting heterogeneous precipitation of the reactive colloids. The precursor concentrations were C_v=0.3 mol/l and 0.145 mol/l and hydrolysis ratio $H=C_w/C_v$ varied between 1.0 and 2.5, where C_V and C_w are concentration of vanadium precursor and water. The series of experiments were repeated. In experiments of VTOA mixed oxides preparation, titanium tetraisopropoxide (TTIP, 98%, Sigma-Aldrich) was used as the precursor of Ti-containing species. Each solution A and B were transferred in glass syringes of a volume 50 ml to the reactor containers maintained under dry nitrogen gas flow, in order to prevent any contamination of the reactive media from the atmosphere. The preparation and transfer of the reactive solutions took from about 20 to 40 minutes. The preparation of the reactive medium was achieved by a simultaneous injection of the stock solutions A and B in a static T-mixer with exocentric input arms of 1 mm diameter and an output tube of 2 mm diameter. The injection was triggered by applying a dry nitrogen gas pressure to the reactor containers by synchronous valves opening. The injected fluids flow with a rate of 10 m/s (at the applied pressure of 4 bar) exhibited a strong turbulence through the mixed zone with a Reynolds number $Re=4Qp/\pi\eta d$, equal to 6000, where Q, p and η are flow rate, density and dynamic viscosity of the fluid respectively, which forces the solutions to mix at the molecular level. The reactor was maintained at the temperature of 20 °C with a thermo-cryostat Haake DC10K15. The optimal operating regime of the sol-gel reactor is attributed to the Damköhler number Da≤1, which means that the time of the fluid composition homogenized before the chemical reactions complete nucleation of species, which permits the narrowest polydispersity of the produced nanoparticles.

2.2 Material characterization

Dynamic Light Scattering (DLS) method was used for the particle size measurements. A home-made monomode optical fiber probe was introduced in the reaction volume to monitor scattered light from a volume ~10^{-6} cm^3, which avoided multiple scattering events and allowed measurements in concentrated solutions. A 40 mW/640 nm single-frequency laser Cube 640-40 Circular (*Coherent*) was used as a coherent light source and signal was analyzed with 48 bits 288 channels photon correlator Photocor-PC2 (*Photocor Instruments*). Each mean radius was obtained from the least-squared fit of the respective autho-correlation curve (ACF) accumulated during 60 s. The confidence range of the experimental was evaluated from spread of R(t) points.
Thermal studies of the vanadium oxide nanopowders were done on a SETARAM TG-DTA 92 device operating simultaneously in thermal gravimetric analysis (TGA) and differential thermal analysis (DTA) in the following conditions: powders of a mass between 40 and 50 mg were introduced into the sample holder and then heated from 50°C to 1000°C with a rising speed of 10°C per minute under argon gas (1 bar). X-ray diffraction (XRD) patterns of powders after heat treatment during 4 hours were analyzed with a benchtop X-ray diffractometer (EQUINOX 1000-Inel) with CoKα source (λ=0.1788976 nm). The prepared samples were characterized using a Zeiss Supra 40 VP SEM-FEG scanning electron microscopy (SEM). The microscopy was performed in a high vacuum mode and low acceleration voltage.

3. Results and Discussion

Before addressing the mixed-oxide system, the nucleation-growth process of the single oxides has to be documented as a reference point. The similar approach has already proven its effectiveness in studies of $Zr_xTi_{1-x}O_2$ solids in a broad range of compositions 0≤x≤1 (Cheng et al. 2017a). The nucleation-growth of titanium-oxo-alkoxy (TOA) species has been previously reported (Azouani et al., 2010; Cheng et al. 2017b). In

the same time, no related information concerning VOA species is available in literature. First observation of the nucleation-growth process of VOA species is presented below.
As it has been shown, inhomogeneous reaction conditions of the sol-gel process generally lead to the appearance of strongly polydispersed species. In contrast, point-like reaction conditions in chemical reactors with ultrarapid (t<10 ms) micromixing permit the process with low Damköhler numbers (Da≤1) resulting in the formation of size selected nanoparticles, among which a nucleus (basic unit of the growing solids) can be firmly identified. For example, DLS and TEM measurements have evidenced the basic TOA unit with radius of R_{TOA}=1.6 nm (Cheng at al., 2017b). Because only general information exists about reactivity of metal-oxo-alkoxy species (Livage at al., 1988), different injection conditions in a T-mixer were tried, leading to the nucleation of VOA species. The size evolution of VOA species prepared manually and in the reactor at different Reynolds numbers (Re) of the injected fluids is shown respectively in Figures 1a and 1b.

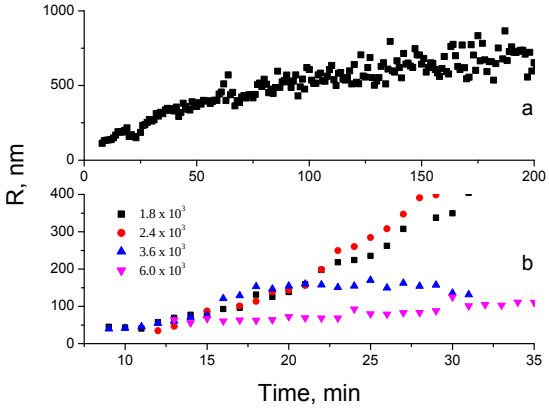

Figure 1: Mean radius of VOA particles prepared manually (a) and in micromixing reactor (b) with different Reynolds numbers (inset) of the injected reactive fluids (C_V=0.30 mol/l, H=1.9, 20 °C).

As one can see, the radius of VOA particles prepared manually evolves from ~120 nm at the beginning to ~1 μm at the precipitation point. In contrast, the VOA particles prepared in the reactor are significantly smaller and have R_0=40 nm after injection; however, their growth kinetics depends on Re value. For relatively low Re<3.6·10^3 the particles grow up to ~1 μm and precipitate (like with manual preparation), while at higher Re the particles remain much finer (R<100 nm) and stable for a long time (days) in colloids. This may infer the homogeneous nucleation of VOA species. We therefore concluded that Re=6·10^3 correspond to the criteria of Da≤1 and conduct further experiments in these injection conditions. The zoom on the very process beginning permits to define a VOA nucleus that begins the growth process: the extrapolation of experimental kinetics in Figure 2a to a common starting point provides the particle radius of R_0=20 nm. The VOA growth kinetics confirms mechanism of the sol-gel process earlier validated on Ti, Zr and Ti-Zr oxo-alkoxy species (Rivallin et al., 2005; Azouani at al., 2007; Labidi et al., 2015; Cheng et al., 2017a). The induction stage takes place at H above a critical value h^*, which is apparently smaller than the experimental values 1.80, … 2.20 (Figure 2b).

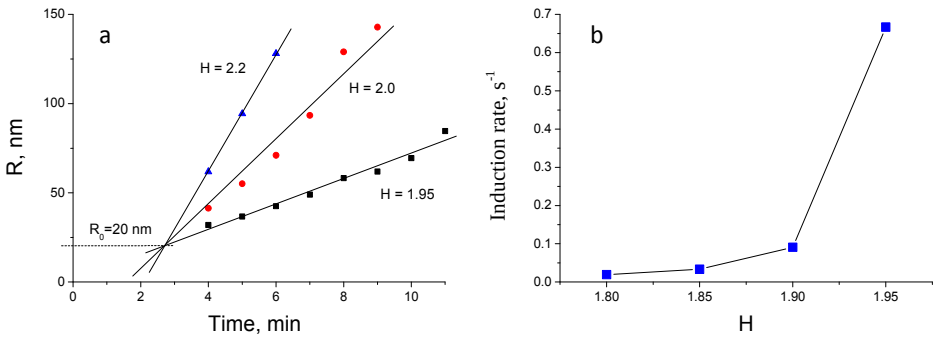

Figure 2: Growth kinetics of VOA nanoparticles in micromixing reactor: particle size versus time for different H (a) and induction rate versus H (b) (C_V = 0.30 mol/l, 20 °C, Re=6000).

The SEM images evidence morphological differences of VOA powders prepared manually (Figure 3a) and in micromixing conditions (Figure 3b), consisting in significantly smaller size of the last, which is in agreement with the DLS observations.

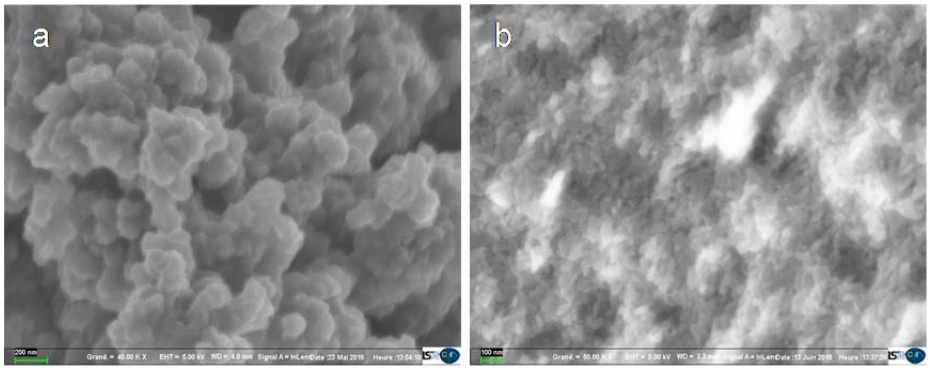

Figure 3: SEM images of VOA nanopowders prepared manually (a) and in micromixing reactor (b) (C_V=0.30 mol/l, H=2.0, heat treatment at T=300 °C for 4 h).

The TGA-DTA measurements in Figure 4a confirm results of vanadium oxides structural evolution. The mass loss of ~17 wt% are connected to the departure of surface alkoxy and hydroxyl groups at T<300 °C. The exothermic peak at 280 °C corresponds to VOA particles crystallization into V_2O_5 metal oxide and the endothermic peak at 675 °C corresponds to the crystalline material melting.

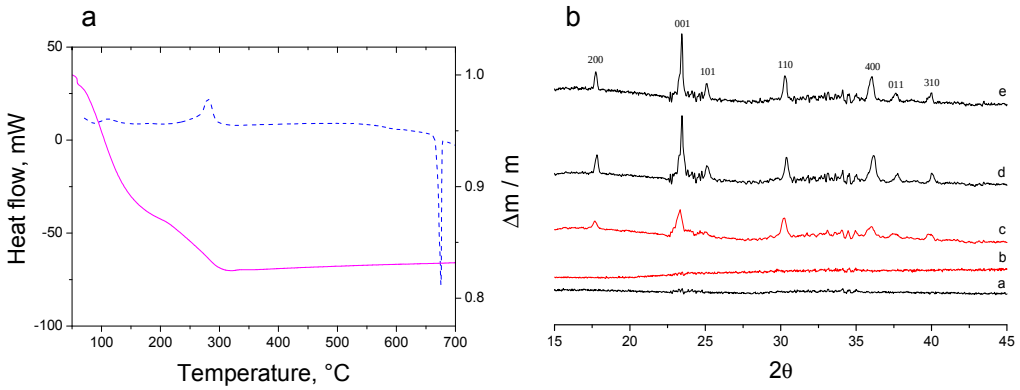

Figure 4: TGA-DTA (a) measurements of VOA powders prepared in the reactor (C_V=0.15 mol/l, H=15, 20 °C, Re=6000) and XRD patterns (b) of V_2O_5 powder prepared manually (a-d) and in micromixing reactor (e) heat treated at 25 °C (a), 200 °C (b), 300 °C (c, e) and 600 °C (d).

The XRD patterns in Figure 4b evidence structural changes of VOA powders. The powders remain amorphous at temperatures T≤200 °C and show crystalline peaks at 300 °C and higher temperatures, which corresponds to the orthorhombic phase of V_2O_5 (JCPDS 01-089-0612). The diffraction peaks become sharper after the heat treatment at a higher temperature, indicating crystalline domains growth. However, narrower peaks were also observed in nanopowders prepared in the micromixing reactor at the crystallization onset (Figure 4e). This may be explained by an easy thermal fusion of small VOA nanoparticles and connected to the morphological modification of the material.

Afterwards, the first synthesis of mixed-oxide VTOA nanoparticles in micromixing conditions was carried out. The measured autho-correlation curves (ACF) in reactive media containing pure V and V-Ti precursors are shown in Figure 5. The ACF in the mixture Ti:V=0.05:0.95 (Figure 5a) fitted with two-exponential decay indicates the bimodal population with particle sizes of R_1=7.9 nm and 75 nm. Comparing the respective amplitudes A_1 and A_2 and taking into account that the scattering light intensity $I \propto R^6$ in the Rayleigh domain of particle sizes, one can conclude the population ratio $p(R_1) / p(R_2) \approx 2 \cdot 10^6$, which shows a strong preference of the small nanoparticles formation in the reaction conditions. In contrast, removal of Ti precursor in similar

reaction conditions (Figure 5b) results in a very weak (noisy) signal corresponding to rare particles of radius R_0=160 nm. We also notice that using pure Ti precursor in similar reaction conditions lead to the formation of monodispersed TOA particles of radius 1.6 nm (Azouani at al., 2007). The observed difference indicates a strong interaction between the two V and Ti systems apparently leading to the nucleation of mixed oxide VTOA nanoparticles. Most probably, because of the strong reactivity and rapid formation, Ti species nucleate first and serve condensation centers for V species.

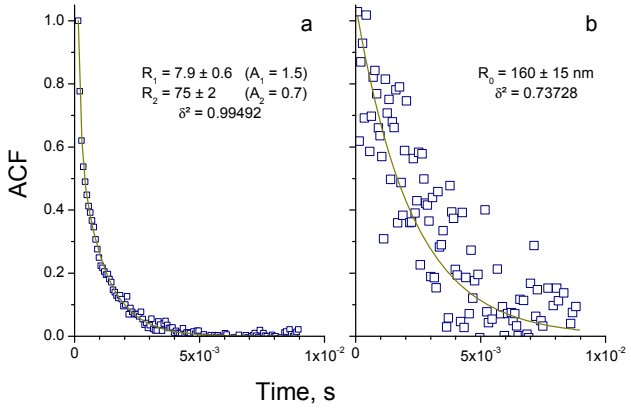

Figure 5: ACF curves of VTOA (a) and VOA (b) nanoparticles in reactive solutions: C_{Ti}=0.285 mol/l, C_V=0.015 mol/l (a) and C_{Ti}=0 mol/l, C_V=0.015 mol/l (b) (H=1.6, n-propanol solvent, 20°C).

The interaction between the vanadium and titanium systems can be confirmed by TGA-DTA measurements of VTOA nanopowder shown in Figure 6. In fact, the exothermic peak of the amorphous-anatase phase transition appears at 505 °C, which is significantly higher than that 380 °C observed in pure titania nanopowders.

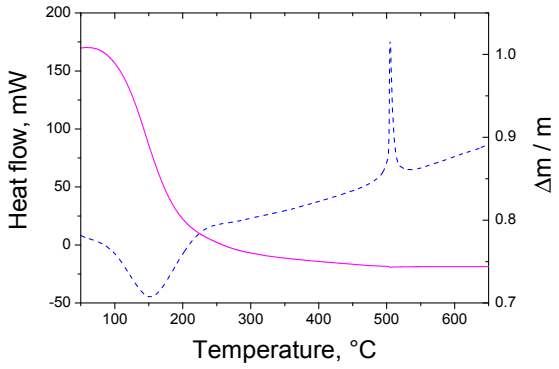

Figure 6: TGA-DTA measurements of VTOA powders with elemental ratio Ti:V=0.9:0.1.

4. Conclusions

This communication is devoted to a critical step in the preparation of mixed-oxide photocatalysts with a homogeneous composition at nanoscale. The nucleation-growth process of vanadium-oxo-alkoxy (VOA) and vanadium-titanium-oxo-alkoxy (VTOA) species was studied in a chemical reactor with an ultra-rapid mixing of the reactive medium. It was shown that the micromixing has a strong impact on the material morphology and structure. First evidence of the formation of VTOA nanoparticles was given. At small hydrolysis ration, VTOA seems to form starting with titanium oxo-alkoxy (TOA) species, which grow by consuming small hydrolyzed VOA species. The optimization of this process is under way.

Acknowledgments

Miguel Sanchez is grateful to CONACYT for the financial support of his PhD work.

References

Amano F., Tanaka T. and Funabiki T., 2004, Steady-state photocatalytic epoxidation of propene by O_2 over V_2O_5/SiO_2 photocatalysts, Langmuir, 20, 4236-4240.

Azouani R., Soloviev A., M. Benmami, Chhor K., Bocquet J.-F., and Kanaev A., 2007, Stability and growth of titanium-oxo-alcoxy $Ti_xO_y(OiPr)_z$ clusters, J. Phys. Chem. C, 111, 16243-6248.

Azouani R., Tieng S., Michau A. , Hassouni K., Chhor K., Bocquet J.-F., Vignes J.-L. and Kanaev A., 2009, Elaboration of Doped and composite nano-TiO_2, Chem. Eng. Trans., 17, 981-986.

Azouani R., Michau A., Hassouni K., Chhor K., Bocquet J-F., Vignes J-L. and Kanaev A., 2010, Elaboration of pure and doped TiO_2 nanoparticles in sol-gel reactor with turbulent micromixing: Application to nanocoatings and photocatalysis, Chem. Eng. Res. Des., 88, 1123-1130.

Cheng K., Chhor K., Brinza O., Vrel D., and Kanaev A., 2017a, From nanoparticles to bulk crystalline solid: Nucleation, growth kinetics and crystallisation of mixed oxide $Zr_xTi_{1-x}O_2$ nanoparticles, Cryst. Eng. Comm., 19, 3955-3965.

Cheng K., Chor K. and Kanaev A., 2017b, Solvent effect on nucleation-growth of titanium-oxo-alkoxy nanoparticles, Chem. Phys. Lett., 672, 119-123.

Cheng K., Chhor K., and Kanaev A., 2018, Photocatalytic nanoparticulate $Zr_xTi_{1-x}O_2$ coatings with controlled homogeneity of elemental composition, Chem. Select, 3, 11118-11126.

Chianese, S., Lovino, P., Leone, V., Musmarra, D. and Prisciandaro, M., 2017, Photodegradation of diclofenac sodium salt in water solution: Effect of HA, NO_3^- and TiO_2 on photolysis performance, Water, Air, and Soil Pollution, 228, 270.

Fagan R., McCormack D.E., Dionysiou D.D., and Pillai S.C., 2016, A review of solar and visible light active TiO_2 photocatalysis for treating bacteria, cyanotoxins and contaminants of emerging concern, Mater. Sci. Semicond. Proc., 42, 2-14.

Fox M. A. and Dulay M. T., 1993, Heterogeneous photocatalysis, Chem. Rev., 93, 341-357.

Hashimoto K., Irie H. and Fujishima A., 2005, TiO_2 photocatalysis: A historical overview and future prospects, Jap. J. Appl. Phys., 44, 8269-8285.

Lovino, P., Chianese, S., Prisciandaro, M. and Musmarra, D., 2019, Triclosan photolysis: operating condition study and photo-oxidation pathway, Chem. Eng. J., doi: 10.1016/j.cej.2019.02.132.

Jianhua L., Rong Y. and Songmei L., 2006, Preparation and Characterization of the TiO_2/V_2O_5 photocatalyst with visible light activity, Rare Metals., 25, 636-642.

Kruefu V., Sintuya H., Pookmanee P. and Phanichphant S., 2017, Visible light photocatalytic degradation of methylene blue using V2O5 nanoparticles, Proc. 6th Int. Conf. Devel. Eng. Technol., Bangkok, Thailand 6-7 February, 62-67.

Labidi S., Jia Z., Ben Amar M., Chhor K. and Kanaev A., 2015, Nucleation and growth kinetics of zirconium-oxo-alkoxy nanopparticles, Phys. Chem. Chem. Phys. 17, 2651-2659.

Li B., Xu Y., Rong G., Jing M. and Xie Y., 2006, Vanadium pentoxide nanobelts and nanorolls: from controllable synthesis to investigation of their electrochemical properties and photocatalytic activities, IOP Publ. Ltd., 17, 2560-2566.

Livage, J., Henry, M. and Sanchez, C., 1988, Sol-gel chemistry of transition metal oxides, Prog. Solid-State Chem., 18, 259-341.

Ohtani B., 2010, Photocatalysis A to Z - What we know and what we do not know in a scientific sense. J. Photochem. Photobiol. C, 11, 157-178.

Schneider J., Matsuoka M., Takeuchi M., Zhang J., Horiuchi Y., Anpo M. and Bahnemann D.W., 2014, Understanding TiO_2 Photocatalysis: Mechanisms and Materials, Chem. Rev., 114, 9919-9986.

Su J., Zou X-X., Li G-D., Wei X., Yan C., Wang Y-N., Zhao J., Zhou L-J. and Chen J-S., 2011, Macroporous V_2O_5-$BiVO_4$ composites: Effect of heterojunction on the behavior of photogenerated charges, J. Phys. Chem., 115, 8064-8071.

Reddy B.M. and Khan A., 2007, Recent advances on TiO_2-ZrO_2 mixed oxides as catalysts and catalyst supports, Catal. Rev., 47, 257-296.

Rivallin M., Benmami M., Kanaev A. and Gaunand A., 2005, Sol–Gel reactor with rapid micromixing: modelling and measurements of titanium oxide nano-particle growth, Chem. Eng. Res. Des., 83, 67-74.

Teramura K., Ohuchi T., Shishido T. and Tanaka T., 2009, Study of the reaction mechanism of selective photooxidation of cyclohexane over V_2O_5/Al_2O_3, J. Phys. Chem., 113, 17018-17024

Tieng S., Kanaev A. and Chhor K., 2011, New homogeneously doped Fe(III)-TiO_2 photocatalyst for gaseous pollutant degradation, Appl. Catal. A, 399, 191-197.

Yang Y., Mao H., Chen H.L. and Selleby M. 2017, An assessment of the Ti-V-O system, J. Alloys Compounds, 722, 365-374.